ФИЗИКА ЭЛЕМЕНТАРНЫХ ЧАСТИЦ И АТОМНОГО ЯДРА
2011. Т. 42. ВЫП. 4

DOUBLE-BETA DECAY EXPERIMENTS

A. S. Barabash

Institute of Theoretical and Experimental Physics, Moscow

ФИЗИКА ЭЛЕМЕНТАРНЫХ ЧАСТИЦ И АТОМНОГО ЯДРА
2011. Т. 42. ВЫП. 4

DOUBLE-BETA DECAY EXPERIMENTS

A. S. Barabash

Institute of Theoretical and Experimental Physics, Moscow

The present status of double-beta decay experiments is reviewed. The results of the most sensitive experiments are discussed. Proposals for future double-beta decay experiments with a sensitivity to the $\langle m_\nu \rangle$ at the level of 0.01–0.1 eV are considered.

PACS: 23.40-s; 14.60.Pq

INTRODUCTION

Interest in neutrinoless double-beta decay has seen a significant renewal in recent years after evidence for neutrino oscillations was obtained from the results of atmospheric, solar, reactor and accelerator neutrino experiments (see, for example, the discussions in [1–3]). These results are impressive proof that neutrinos have a nonzero mass. However, the experiments studying neutrino oscillations are not sensitive to the nature of the neutrino mass (Dirac or Majorana) and provide no information on the absolute scale of the neutrino masses, since such experiments are sensitive only to the difference of the masses, Δm^2. The detection and study of $0\nu\beta\beta$ decay may clarify the following problems of neutrino physics (see discussions in [4–6]): (i) lepton number nonconservation, (ii) neutrino nature: whether the neutrino is a Dirac or a Majorana particle, (iii) absolute neutrino mass scale (a measurement or a limit on m_1), (iv) the type of neutrino mass hierarchy (normal, inverted, or quasidegenerate), (v) CP violation in the lepton sector (measurement of the Majorana CP-violating phases).

Let us consider three main modes of 2β decay:

$$(A, Z) \to (A, Z+2) + 2e^- + 2\bar{\nu}, \tag{1}$$

$$(A, Z) \to (A, Z+2) + 2e^-, \tag{2}$$

$$(A, Z) \to (A, Z+2) + 2e^- + \chi^0 (+\chi^0). \tag{3}$$

The $2\nu\beta\beta$ decay (process (1)) is a second-order process, which is not forbidden by any conservation law. The detection of this process provides the experimental determination of the nuclear matrix elements (NME) involved in the double-beta decay processes. This leads to the development of theoretical

schemes for NME calculations both in connection with the $2\nu\beta\beta$ decays as well as the $0\nu\beta\beta$ decays [7–10]. Moreover, the study can yield a careful investigation of the time dependence of the coupling constant for weak interactions [11–13].

Recently, it has been pointed out that the $2\nu\beta\beta$ decay allows one to investigate particle properties, in particular whether the Pauli exclusion principle is violated for neutrinos and thus neutrinos partially obey Bose–Einstein statistics [14, 15].

The $0\nu\beta\beta$ decay (process (2)) violates the law of lepton-number conservation ($\Delta L = 2$) and requires that the Majorana neutrino has a nonzero rest mass. Also, this process is possible in some supersymmetric models, where $0\nu\beta\beta$ decay is initiated by the exchange of supersymmetric particles. This decay also arises in models featuring an extended Higgs sector within electroweak-interaction theory and in some other cases [16].

The $0\nu\chi^0\beta\beta$ decay (process (3)) requires the existence of a Majoron. It is a massless Goldstone boson that arises due to a global breakdown of $(B-L)$ symmetry, where B and L are, respectively, the baryon and the lepton number. The Majoron, if it exists, could play a significant role in the history of the early Universe and in the evolution of stars. The model of a triplet Majoron [17] was disproved in 1989 by the data on the decay width of the Z^0 boson that were obtained at the LEP accelerator [18]. Despite this, some new models were proposed [19,20], where $0\nu\chi^0\beta\beta$ decay is possible and where there are no contra-

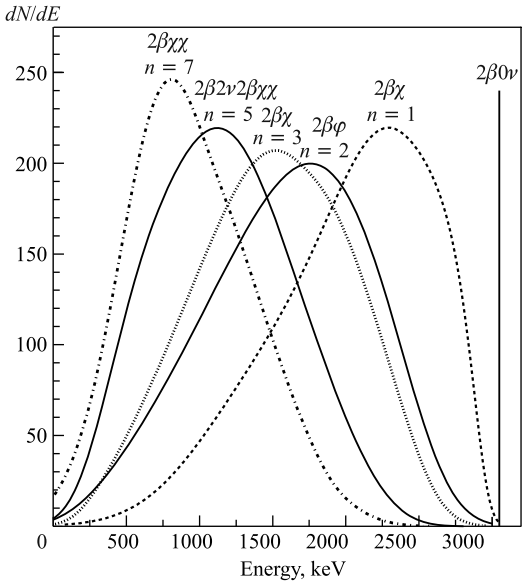

Fig. 1. Energy spectra of different modes of $2\nu\beta\beta$ ($n = 5$), $0\nu\chi^0\beta\beta$ ($n = 1, 2$, and 3) and $0\nu\chi^0\chi^0\beta\beta$ ($n = 3$ and 7) decays of ^{100}Mo

dictions with the LEP data. A 2β-decay model that involves the emission of two Majorons was proposed within supersymmetric theories [21], and several other models of the Majoron were proposed in the 1990s. By the term «Majoron», one means massless or light bosons that are associated with neutrinos. In these models, the Majoron can carry a lepton charge and is not required to be a Goldstone boson [22]. A decay process that involves the emission of two «Majorons» is also possible [23]. In models featuring a vector Majoron, the Majoron is the longitudinal component of a massive gauge boson emitted in 2β decay [24]. For the sake of simplicity, each such object is referred to here as a Majoron. In [25], a «bulk» Majoron model was proposed in the context of the «brane-bulk» scenario for particle physics.

The possible two electrons energy spectra for different 2β-decay modes of ^{100}Mo are shown in Fig. 1. Here *n* is the spectral index, which defines the shape of the spectrum. For example, for an ordinary Majoron $n = 1$; for 2ν decay, $n = 5$, in the case of a bulk Majoron $n = 2$ and for the process with two Majorons emission $n = 3$ or 7.

1. RESULTS OF EXPERIMENTAL INVESTIGATIONS

The number of possible candidates for double-beta decay is quite large, there are 35 nuclei*. However, nuclei for which the double-beta transition energy ($E_{2\beta}$) is in excess of 2 MeV are of the greatest interest, since the double-beta decay probability strongly depends on the transition energy ($\sim E_{2\beta}^{11}$ for $2\nu\beta\beta$ decay, $\sim E_{2\beta}^{7}$ for $0\nu\chi^0\beta\beta$ decay and $\sim E_{2\beta}^{5}$ for $0\nu\beta\beta$ decay). In transitions to excited states of the daughter nucleus, the excitation energy is removed via the emission of one or more photons, which can be detected, and this can serve as an additional source of information about double-beta decay. As an example Fig. 2 shows the diagram of energy levels in the ^{100}Mo–^{100}Tc–^{100}Ru nuclear triplet.

1.1. Two-Neutrino Double-Beta Decay. This decay was first recorded in 1950 in a geochemical experiment with ^{130}Te [27]; in 1967, $2\nu\beta\beta$ decay was found for ^{82}Se also in a geochemical experiment [28]. Attempts to observe this decay in a direct experiment employing counters had been futile for a long time. Only in 1987 could M. Moe, who used a time-projection chamber (TPC), observe $2\nu\beta\beta$ decay in ^{82}Se for the first time [29]. In the next few years, experiments were able to detect $2\nu\beta\beta$ decay in many nuclei. In ^{100}Mo and ^{150}Nd $2\beta(2\nu)$ decay to the 0^+ excited state of the daughter nucleus was measured, too (see [30]). Also, the $2\nu\beta\beta$ decay of ^{238}U was detected in a radiochemical experiment [31], and in a geochemical experiment the ECEC process was detected in ^{130}Ba (see

*In addition 34 nuclei can undergo double-electron capture, while twenty two nuclei and six nuclei can undergo, respectively, ECβ^+ and $2\beta^+$ decay (see the tables in [26]).

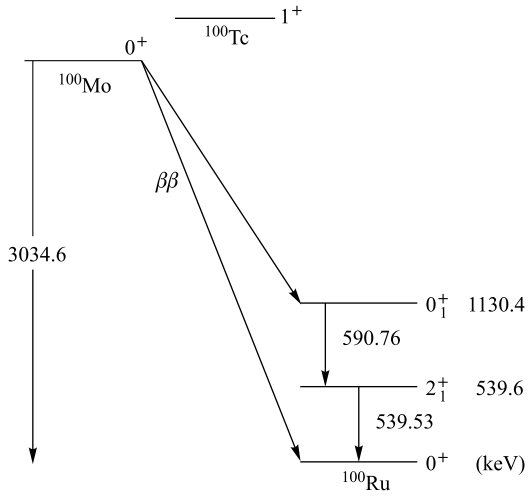

Fig. 2. Levels scheme for ^{100}Mo–^{100}Tc–^{100}Ru

Table 1. **Averaged and recommended $T_{1/2}(2\nu)$ values (from [30])**

Isotope	$T_{1/2}(2\nu)$, y
^{48}Ca	$4.4^{+0.6}_{-0.5} \cdot 10^{19}$
^{76}Ge	$(1.5 \pm 0.1) \cdot 10^{21}$
^{82}Se	$(0.92 \pm 0.07) \cdot 10^{20}$
^{96}Zr	$(2.3 \pm 0.2) \cdot 10^{19}$
^{100}Mo	$(7.1 \pm 0.4) \cdot 10^{18}$
^{100}Mo–^{100}Ru(0^+_1)	$(5.9^{+0.8}_{-0.6}) \cdot 10^{20}$
^{116}Cd	$(2.8 \pm 0.2) \cdot 10^{19}$
^{128}Te	$(1.9 \pm 0.4) \cdot 10^{24}$
^{130}Te	$(6.8^{+1.2}_{-1.1}) \cdot 10^{20}$
^{150}Nd	$(8.2 \pm 0.9) \cdot 10^{18}$
^{150}Nd–^{150}Sm(0^+_1)	$1.33^{+0.45}_{-0.26} \cdot 10^{20}$
^{238}U	$(2.0 \pm 0.6) \cdot 10^{21}$
^{130}Ba; ECEC(2ν)	$(2.2 \pm 0.5) \cdot 10^{21}$

Subsec. 1.4). Table 1 displays the present-day averaged and recommended values of $T_{1/2}(2\nu)$ from [30]. At present, experiments devoted to detecting $2\nu\beta\beta$ decay are approaching a level where it is insufficient to just record the decay. It is necessary to measure numerous parameters of this process to a high precision (energy sum spectrum, single-electron energy spectrum and angular distribution). Tracking detectors that are able to record both the energy of each electron and

Table 2. **Best present results on $0\nu\beta\beta$ decay (limits at 90% CL)**

Isotope ($E_{2\beta}$, keV)	$T_{1/2}$, y	$\langle m_\nu \rangle$, eV [7–10]	$\langle m_\nu \rangle$, eV [39]	Experiment
^{76}Ge (2039)	$> 1.9 \cdot 10^{25}$	<0.22–0.41	< 0.69	HM [41]
	$\simeq 1.2 \cdot 10^{25}$(?)	$\simeq$ 0.28–0.52(?)	$\simeq 0.87$(?)	Part of HM [32]
	$\simeq 2.2 \cdot 10^{25}$(?)	$\simeq$ 0.21–0.38(?)	$\simeq 0.64$(?)	Part of HM [33]
	$> 1.6 \cdot 10^{25}$	<0.24–0.44	< 0.75	IGEX [42]
^{130}Te (2529)	$> 3 \cdot 10^{24}$	<0.29–0.57	< 0.75	CUORICINO [43]
^{100}Mo (3034)	$> 1.1 \cdot 10^{24}$	<0.45–0.93	—	NEMO-3* [44]
^{136}Xe (2458)	$> 4.5 \cdot 10^{23}$**	<1.14–2.68	< 2.2	DAMA [45]
^{82}Se (2995)	$> 3.6 \cdot 10^{23}$	<0.89–1.61	< 2.3	NEMO-3* [44]
^{116}Cd (2805)	$> 1.7 \cdot 10^{23}$	<1.40–2.76	< 1.8***	SOLOTVINO [46]

*Current experiments.
**Conservative limit from [45] is presented.
***NME from [40] is used.

the angle at which they diverge are the most appropriate instruments for solving this problem.

1.2. Neutrinoless Double-Beta Decay. In contrast to two-neutrino decay, neutrinoless double-beta decay has not yet been observed*, although it is easier to detect it. In this case, one seeks, in the experimental spectrum, a peak of energy equal to the double-beta transition energy and of width determined by the detector's resolution.

The constraints on the existence of $0\nu\beta\beta$ decay are presented in Table 2 for the nuclei that are the most promising candidates. In calculating constraints on $\langle m_\nu \rangle$, the nuclear matrix elements from [7–10] were used (3rd column). It is advisable to employ the calculations from these studies, because the calculations are the most thorough and take into account the most recent theoretical achievements. In these papers, g_{pp} values (g_{pp} is a parameter of the QRPA theory) were fixed using experimental half-life values for 2ν decay and then NME(0ν) were calculated. In column four, limits on $\langle m_\nu \rangle$, which were obtained using the NMEs from a recent Shell Model (SM) calculations [39], are presented (for ^{116}Cd NME from [40] is used).

*The possible exception is the result with ^{76}Ge, published by a fraction of the Heidelberg–Moscow Collaboration, $T_{1/2} \simeq 1.2 \cdot 10^{25}$ y [32] or $T_{1/2} \simeq 2.2 \cdot 10^{25}$ y [33]. For the first time the «positive» result was mentioned in [34]. The Moscow part of the Collaboration does not agree with this conclusion [35] and there are others who are critical of this result [36–38]. Thus, at the present time, this «positive» result is not accepted by the «2β-decay community» and it has to be checked by new experiments.

From Table 2 using NME values from [7–10], the limits on $\langle m_\nu \rangle$ for ^{130}Te are comparable with the ^{76}Ge results. Now one cannot select any experiment as the best one. The assemblage of sensitive experiments for different nuclei permits one to increase the reliability of the limit on $\langle m_\nu \rangle$. Present conservative limit can be set as 0.75 eV.

1.3. Double-Beta Decay with Majoron Emission. Table 3 displays the best present-day constraints for an «ordinary» Majoron ($n = 1$). The NME from the following works were used, 3rd column: [7–10], 4th column: [39]. The «non-standard» models of the Majoron were experimentally tested in [49] for ^{76}Ge and in [50] for ^{100}Mo, ^{116}Cd, ^{82}Se, and ^{96}Zr. Constraints on the decay modes involving the emission of two Majorons were also obtained for ^{100}Mo [51], ^{116}Cd [46], and ^{130}Te [52]. In a recent NEMO Collaboration papers, new results for these processes in ^{100}Mo [47], ^{82}Se [47], ^{150}Nd [53], and ^{96}Zr [54] were obtained with the NEMO-3 detector. Table 4 gives the best experimental constraints on decays accompanied by the emission of one or two Majorons (for $n = 2, 3$, and 7). Hence, at the present time, only limits on double-beta decay with Majoron emission have been obtained (see Tables 3 and 4). A conservative present limit on the coupling constant of ordinary Majoron to the neutrino is $\langle g_{ee} \rangle < 1.9 \cdot 10^{-4}$.

Table 3. **The best present limits on $0\nu\chi^0\beta\beta$ decay (ordinary Majoron) at 90% CL**

Isotope ($E_{2\beta}$, keV)	$T_{1/2}$, y	$\langle g_{ee} \rangle$ [7–10]	$\langle g_{ee} \rangle$ [39]
^{76}Ge (2039)	$> 6.4 \cdot 10^{22}$ [41]	$< (0.54\text{–}1.44) \cdot 10^{-4}$	$< 2.4 \cdot 10^{-4}$
^{82}Se (2995)	$> 1.5 \cdot 10^{22}$ [47]	$< (0.58\text{–}1.19) \cdot 10^{-4}$	$< 1.9 \cdot 10^{-4}$
^{100}Mo (3034)	$> 2.7 \cdot 10^{22}$ [47]	$< (0.35\text{–}0.85) \cdot 10^{-4}$	—
^{116}Cd (2805)	$> 8 \cdot 10^{21}$ [46]	$< (0.79\text{–}2.56) \cdot 10^{-4}$	$< 1.7 \cdot 10^{-4}$**
^{128}Te (867)	$> 1.5 \cdot 10^{24}$(geochem.) [30, 48]	$< (0.63\text{–}1) \cdot 10^{-4}$	$< 1.4 \cdot 10^{-4}$
^{136}Xe (2458)	$> 1.6 \cdot 10^{22}$* [45]	$< (1.51\text{–}3.54) \cdot 10^{-4}$	$< 2.9 \cdot 10^{-4}$

*Conservative limit from [45] is presented.
**NME from [40] is used.

1.4. $2\beta^+$, ECβ^+, and ECEC Processes. Much less attention has been given to the investigation of $2\beta^+$, β^+EC, and ECEC processes, although such attempts were done from time to time in the past (see review [55]). Again, the main interest here is connected with neutrinoless decay:

$$(A, Z) \to (A, Z-2) + 2e^+, \tag{4}$$

$$e^- + (A, Z) \to (A, Z-2) + e^+ + X, \tag{5}$$

$$e^- + e^- + (A, Z) \to (A, Z-2)^* \to (A, Z-2) + \gamma + 2X. \tag{6}$$

Table 4. **The best present limits on $T_{1/2}$ for decay with one and two Majorons at 90% CL for modes with spectral index $n = 2$, $n = 3$ and $n = 7$**

Isotope ($E_{2\beta}$, keV)	n = 2	n = 3	n = 7
^{76}Ge (2039)	—	$> 5.8 \cdot 10^{21}$ [49]	$> 6.6 \cdot 10^{21}$ [49]
^{82}Se (2995)	$> 6 \cdot 10^{21}$ [47]	$> 3.1 \cdot 10^{21}$ [47]	$> 5 \cdot 10^{20}$ [47]
^{96}Zr (3350)	$> 9.9 \cdot 10^{20}$ [54]	$> 5.8 \cdot 10^{20}$ [54]	$> 1.1 \cdot 10^{20}$ [54]
^{100}Mo (3034)	$> 1.7 \cdot 10^{22}$ [47]	$> 1 \cdot 10^{22}$ [47]	$> 7 \cdot 10^{19}$ [47]
^{116}Cd (2805)	$> 1.7 \cdot 10^{21}$ [46]	$> 8 \cdot 10^{20}$ [46]	$> 3.1 \cdot 10^{19}$ [46]
^{130}Te (2529)	—	$> 9 \cdot 10^{20}$ [52]	—
^{128}Te (867) (geochem.)	$> 1.5 \cdot 10^{24}$ [30,48]	$> 1.5 \cdot 10^{24}$ [30,48]	$> 1.5 \cdot 10^{24}$ [30,48]
^{150}Nd (3371)	$> 5.4 \cdot 10^{20}$ [53]	$> 2.2 \cdot 10^{20}$ [53]	$> 4.7 \cdot 10^{19}$ [53]

There are 34 candidates for these processes. Only 6 nuclei can undergo all the above-mentioned processes and 16 nuclei can undergo β^+EC and ECEC while 12 can undergo only ECEC. Detection of the neutrinoless mode in the above processes enables one to determine the effective Majorana neutrino mass $\langle m_\nu \rangle$, parameters of right-handed current admixture in electroweak interaction ($\langle \lambda \rangle$ and $\langle \eta \rangle$), etc.

Process (4) has a very nice signature because, in addition to two positrons, four annihilation 511 keV gamma quanta will be detected. On the other hand, the rate for this process should be much lower in comparison with $0\nu\beta\beta$ decay because of substantially lower kinetic energy available in such a transition (2.044 MeV is spent for creation of two positrons) and of the Coulomb barrier for positrons. There are only six candidates for this type of decay: ^{78}Kr, ^{96}Ru, ^{106}Cd, ^{124}Xe, ^{130}Ba, and ^{136}Ce. The half-lives of the most prospective isotopes are estimated to be $\sim 10^{27}$–10^{28} y (for $\langle m_\nu \rangle = 1$ eV) [56, 57]; this is approximately 10^3–10^4 times higher than for $0\nu\beta\beta$ decay for such nuclei as ^{76}Ge, ^{100}Mo, ^{82}Se, and ^{130}Te.

Process (5) has a nice signature (positron and two annihilation 511 keV gammas) and is not as strongly suppressed as $2\beta^+$ decay. In this case, half-life estimates for the best nuclei give $\sim 10^{26}$–10^{27} y (again for $\langle m_\nu \rangle = 1$ eV) [56,57].

In the last case (process (6)), the atom de-excites emitting two X-rays and the nucleus de-excites emitting one γ ray (bremsstrahlung photon)*. For a transition to an excited state of the daughter nucleus, besides a bremsstrahlung photon,

*In fact, the processes with irradiation of inner conversion electron, e^+e^- pair or two gammas are also possible [58] (in addition, see discussion in [59]). These possibilities are especially important in the case of the ECEC(0ν) transition with the capture of two electrons from the *K* shell. In this case the transition with irradiation of one γ is strongly suppressed [58].

γ rays are emitted from the decay of the excited state. Thus, there is a clear signature for this process. The rate is practically independent of decay energy and increases with both decreasing bremsstrahlung photon energy and increasing Z [59,60]. The rate is quite low even for heavy nuclei, with $T_{1/2} \sim 10^{28}$–10^{31} y ($\langle m_\nu \rangle = 1$ eV) [59]. The rate can be increased in $\sim 10^6$ times if resonance conditions exist (see below).

For completeness, let us present the two-neutrino modes of $2\beta^+$, β^+EC, and ECEC processes:

$$(A, Z) \to (A, Z-2) + 2e^+ + 2\nu, \tag{7}$$

$$e^- + (A, Z) \to (A, Z-2) + e^+ + 2\nu + X, \tag{8}$$

$$e^- + e^- + (A, Z) \to (A, Z-2) + 2\nu + 2X. \tag{9}$$

These processes are not forbidden by any conservation laws, and their observation is interesting from the point of view of investigating nuclear-physics aspects of double-beta decay. Processes (7) and (8) are quite strongly suppressed because of low phase-space volume, and investigation of process (9) is very difficult because one only has low energy X-rays to detect. In the case of double-electron capture, it is again interesting to search for transitions to the excited states of daughter nuclei, which are easier to detect experimentally [61]. For the best candidates half-life is estimated as $\sim 10^{27}$ y for $\beta^+\beta^+$, $\sim 10^{22}$ y for β^+EC, and $\sim 10^{21}$ y for ECEC processes [57].

During the last few years, interest in the $\beta^+\beta^+$, β^+EC, and ECEC processes has greatly increased. For the first time a positive result was obtained in a geochemical experiment with ^{130}Ba, where the ECEC(2ν) process was detected with a half-life of $(2.2 \pm 0.5) \cdot 10^{21}$ y [62]. Recently new limits on the ECEC(2ν) process in the promising candidate isotopes (^{78}Kr and ^{106}Cd) were established ($2.4 \cdot 10^{21}$ y [63] and $4.1 \cdot 10^{20}$ y [64], respectively). Very recently β^+EC and ECEC processes in ^{120}Te [65,66], ^{74}Se [67], ^{64}Zn [68,69] and ^{112}Sn [69–71] were investigated. Among the recent papers there are a few new theoretical papers with half-life estimations [56,72–78]. Nevertheless, the $\beta^+\beta^+$, β^+EC, and ECEC processes have not been investigated very well theoretically or experimentally. One can imagine some unexpected results here, which is why any improvements in experimental sensitivity for such transitions has merit.

Table 5 gives a compendium of the best present-day constraints for $2\beta^+$, ECβ^+, and ECEC processes and the result of the geochemical experiment that employed ^{130}Ba and which yields the first indication of the observation of ECEC(2ν) capture.

In [84], for the first time it was mentioned that in the case of ECEC(0ν) transition a resonance condition could exist for transitions to a «right energy» excited state of the daughter nucleus, when the decay energy is close to zero. In 1982, the same idea was proposed for transitions to the ground state [85].

Table 5. **The most significant experimental results for $2\beta^+$, ECβ^+, and ECEC processes (all limits are presented at a 90% CL). Here Q is equal to ΔM (atomic mass difference of parent and daughter nuclei) for ECEC, (ΔM — 1022 keV) for ECβ^+ and (ΔM — 2044 keV) for $2\beta^+$**

Decay type	Nucleus	Q, keV	$T_{1/2}$, y	References
ECEC(0ν)	^{130}Ba	2611	$> 4 \cdot 10^{21}$	[79]
	^{78}Kr	2866	$> 2.4 \cdot 10^{21}$	[63]
	^{132}Ba	839.9	$> 3 \cdot 10^{20}$	[79]
	^{106}Cd	2771	$> 1.6 \cdot 10^{20}$	[64]
ECEC(2ν)	^{130}Ba	2611	$> 4 \cdot 10^{21}$	[79]
			$= 2.1^{+3.0}_{-0.8} \cdot 10^{21}$	[79]
			$= (2.2 \pm 0.5) \cdot 10^{21}$	[62]
	^{78}Kr	2866	$> 2.4 \cdot 10^{21}$	[63]
	^{106}Cd	2771	$> 4.1 \cdot 10^{20}$	[64]
	^{132}Ba	839.9	$> 3 \cdot 10^{20}$	[79]
EC$\beta^+(0\nu)$	^{130}Ba	1589	$> 4 \cdot 10^{21}$	[79]
	^{78}Kr	1844	$> 2.5 \cdot 10^{21}$	[80]
	^{58}Ni	903.8	$> 4.4 \cdot 10^{20}$	[81]
	^{106}Cd	1749	$> 3.7 \cdot 10^{20}$	[82]
	^{92}Mo	627.1	$> 1.9 \cdot 10^{20}$	[83]
EC$\beta^+(2\nu)$	^{130}Ba	1589	$> 4 \cdot 10^{21}$	[79]
	^{58}Ni	903.8	$> 4.4 \cdot 10^{20}$	[81]
	^{106}Cd	1749	$> 4.1 \cdot 10^{20}$	[82]
	^{92}Mo	627.1	$> 1.9 \cdot 10^{20}$	[83]
	^{78}Kr	1844	$> 7 \cdot 10^{19}$	[80]
$2\beta^+(0\nu)$	^{130}Ba	567	$> 4 \cdot 10^{21}$	[79]
	^{78}Kr	822	$> 1 \cdot 10^{21}$	[80]
	^{106}Cd	727	$> 2.4 \cdot 10^{20}$	[82]
$2\beta^+(2\nu)$	^{130}Ba	567	$> 4 \cdot 10^{21}$	[79]
	^{78}Kr	822	$> 1 \cdot 10^{21}$	[80]
	^{106}Cd	727	$> 2.4 \cdot 10^{20}$	[82]

In 1983, this transition was discussed for ^{112}Sn–^{112}Cd (0^+; 1871 keV) [86]. In 2004, the idea was reanalyzed in [59] and new resonance condition for the decay was formulated. The possible enhancement of the transition rate was estimated as $\sim 10^6$ [59,86], which means that the process starts to be competitive with $0\nu\beta\beta$-decay sensitivity to neutrino mass and it is possible to check this by experiment. There are several candidates for such resonance transitions, to the ground (^{152}Gd, ^{164}Eu, and ^{180}W) and to the excited states (^{74}Se, ^{78}Kr, ^{96}Ru,

Table 6. **The best present limits on ECEC(0ν) to the excited state at a 90% CL for isotope-candidates with possible resonance enhancement. Here ΔM is the atomic mass difference of parent and daughter nuclei, $E^*(J^\pi)$ is the energy of the excited state of the daughter nuclide (with its spin and parity in parenthesis)**

Nucleus	Abundance, %	ΔM, keV	$E^*(J^\pi)$	$T_{1/2}$, y
^{74}Se	0.89	1209.240 ± 0.007	1204.2 (2^+)	$> 5.5 \cdot 10^{18}$ [67]
^{78}Kr	0.35	2846.4 ± 2.0	2838.9 (2^+)	$> 1.5 \cdot 10^{21*}$
^{96}Ru	5.52	2718.5 ± 8.2	2700.2 (2^+)	$> 4.9 \cdot 10^{18}$ [90]
			2712.68.1 (?)	$> 1.3 \cdot 10^{19}$ [90]
^{106}Cd	1.25	2770 ± 7.2	2741.0 (4^+)	$> 1.6 \cdot 10^{20}$ [64]
			2748.2 ($2,3^-$)	—
^{112}Sn	0.97	1919.82 ± 0.16	1871.0 (0^+)	$> 4.7 \cdot 10^{20}$ [94]
^{130}Ba	0.11	2617.1 ± 2.0	2608.4 (?)	$> 1.5 \cdot 10^{21**}$
			2544.43 (?)	$> 1.5 \cdot 10^{21**}$
^{136}Ce	0.20	2418.9 ± 13	2399.9 ($1^+,2^+$)	$> 4.1 \cdot 10^{15}$ [91]
			2392.1 ($1^+,2^+$)	$> 2.4 \cdot 10^{15}$ [91]
^{162}Er	0.14	1843.8 ± 5.6	1745.7 (1^+)	—
			1782.68 (2^+)	—

*Extracted from results for the ECEC(2ν; 0^+–0^+_{gs}) transition obtained for ^{78}Kr [63].
**Extracted from geochemical experiments [62, 79].

^{106}Cd, ^{112}Sn, ^{130}Ba, ^{136}Ce, and ^{162}Er) of daughter nuclei. The precision needed to realize resonance conditions is well below 1 keV. To select the best candidate from the above list one will have to know the atomic mass difference with an accuracy better than 1 keV. Unfortunately, by the moment for all mentioned above isotopes the accuracy is mainly on the level of 2–13 keV. In fact, it is possible to know these values with much better accuracy and recently the atomic-mass difference between ^{112}Sn and ^{112}Cd was measured with accuracy 0.16 keV [87] and between ^{74}Se and ^{74}Ge with accuracy 0.007 keV [88] and 0.049 keV [89]*. The experimental search for such a resonance transition in ^{74}Se to ^{74}Ge (2^+; 1206.9 keV) was performed yielding a limit $T_{1/2} > 5.5 \cdot 10^{18}$ y [67]. Recently the limits on the level of $1.6 \cdot 10^{20}$ y, $(0.5 - 1.3) \cdot 10^{19}$ y and $\sim (2 - 4) \cdot 10^{15}$ y for the resonant neutrinoless transitions in ^{106}Cd [64], ^{96}Ru [90], and ^{136}Ce [91] were obtained. Resonance transition in ^{112}Sn was investigated by three different experimental groups using natural and enriched samples of tin [70, 71, 92–94]. The more strong limit of $T_{1/2} > 4.7 \cdot 10^{20}$ y was obtained for the transition to

*Unfortunately, these measurements demonstrate that the strong enhancement scenario for the ^{112}Sn and ^{74}Se decays is disfavored.

the 0^+ state at 1871 keV with the 53 g enriched tin sample [94]. It has also been demonstrated that using enriched ^{112}Sn (or ^{74}Se) at an installation such as GERDA or MAJORANA, a sensitivity on the level $\sim 10^{26}$ y can be reached. The best present limits are presented in Table 6.

2. LARGE-SCALE CURRENT EXPERIMENT NEMO-3 [95–97]

This tracking experiment, in contrast to experiments with ^{76}Ge, detects not only the total energy deposition, but other parameters of the process, including the energy of the individual electrons, angle between them, and the coordinates of the event in the source plane. The performance of the detector was studied with the NEMO-2 prototype [98]. Since June of 2002, the NEMO-3 detector has operated in the Frejus Underground Laboratory (France) located at a depth of 4800 m w.e. The detector has a cylindrical structure and consists of 20 identical sectors (see Fig. 3). A thin (30–60 mg/cm^2) source containing double-beta-decaying nuclei and natural material foils having a total area of 20 m^2 and a weight of up to 10 kg was placed in the detector. The basic principles of detection are identical to those used in the NEMO-2 detector. The energy of the electrons is measured by plastic scintillators (1940 individual counters), while the tracks are reconstructed on the basis of information obtained in the planes of Geiger cells (6180 cells) surrounding the source on both sides. The tracking volume of the detector is filled with a mixture consisting of $\sim$ 95% He, 4% alcohol, 1% Ar, and 0.1% water at slightly above atmospheric pressure. In addition, a magnetic field with a strength of 25 G parallel to the detector's axis is created by a solenoid surrounding the detector. The magnetic field is used to identify electron–positron pairs so as to suppress this source of background.

The main characteristics of the detector are the following. The energy resolution of the scintillation counters lies in the interval 14–17% FWHM for electrons of energy 1 MeV. The time resolution is 250 ps for an electron energy of 1 MeV and the accuracy in reconstructing the vertex of $2e^-$ events is 1 cm. The detector is surrounded by a passive shield consisting of 20 cm of steel and 30 cm of borated water. The level of radioactive impurities in structural materials of the detector and of the passive shield was tested in measurements with low-background HPGe detectors.

Measurements with the NEMO-3 detector revealed that tracking information, combined with time and energy measurements, makes it possible to suppress the background efficiently. That NEMO-3 can be used to investigate almost all isotopes of interest is a distinctive feature of this facility. At the present time, such investigations are being performed for seven isotopes, these are: ^{100}Mo, ^{82}Se, ^{116}Cd, ^{150}Nd, ^{96}Zr, ^{130}Te, and ^{48}Ca (see Table 7). As is mentioned above, foils of copper and natural (not enriched) tellurium were placed in the detector to perform background measurements.

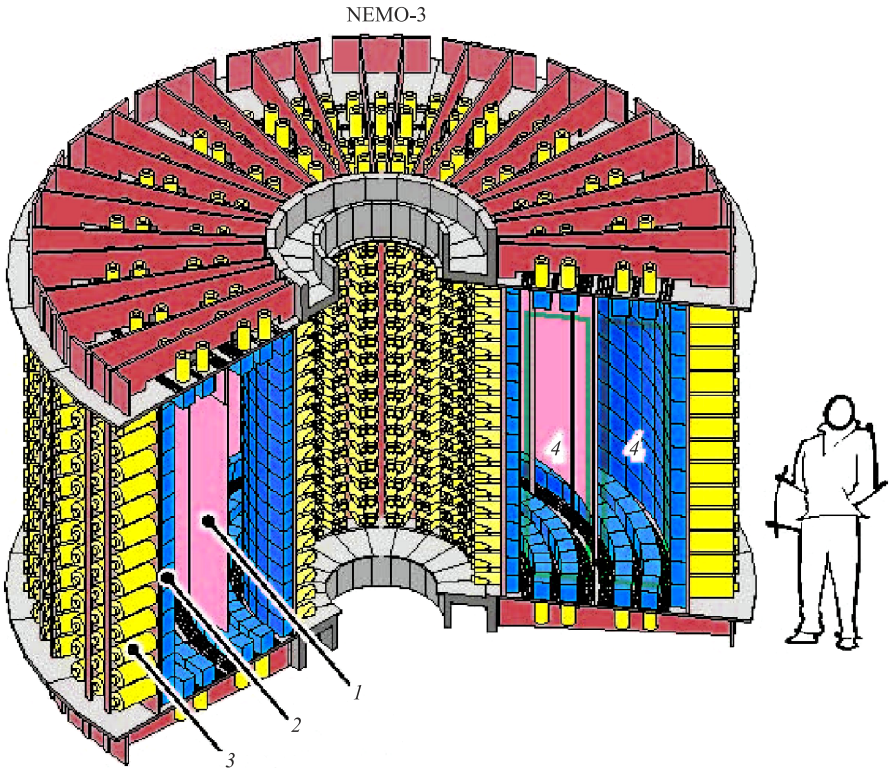

Fig. 3. The NEMO-3 detector without shielding [96]: *1* — source foil; *2* — plastic scintillator; *3* — low radioactivity PMT; *4* — tracking chamber

Table 7. **Isotopes investigated with NEMO-3 [96]**

Isotope	^{100}Mo	^{82}Se	^{130}Te	^{116}Cd	^{150}Nd	^{96}Zr	^{48}Ca
Enrichment, %	97	97	89	93	91	57	73
Mass of isotope, g	6914	932	454	405	36.6	9.4	7.0

Figures 4 and 5 display the spectrum of $2\nu\beta\beta$ events for ^{100}Mo and ^{82}Se that were collected over 389 days (Phase I) [95]. For ^{100}Mo the angular distribution (Fig. 4, *b*) and single-electron spectrum (Fig. 4, *c*) are also shown. The total number of events exceeds 219,000 which is much greater than the total statistics of all the preceding experiments with ^{100}Mo (and even greater than the total statistics of all previous $2\nu\beta\beta$-decay experiments!). It should also be noted that the background is as low as 2.5% of the total number of $2\nu\beta\beta$ events. Employing

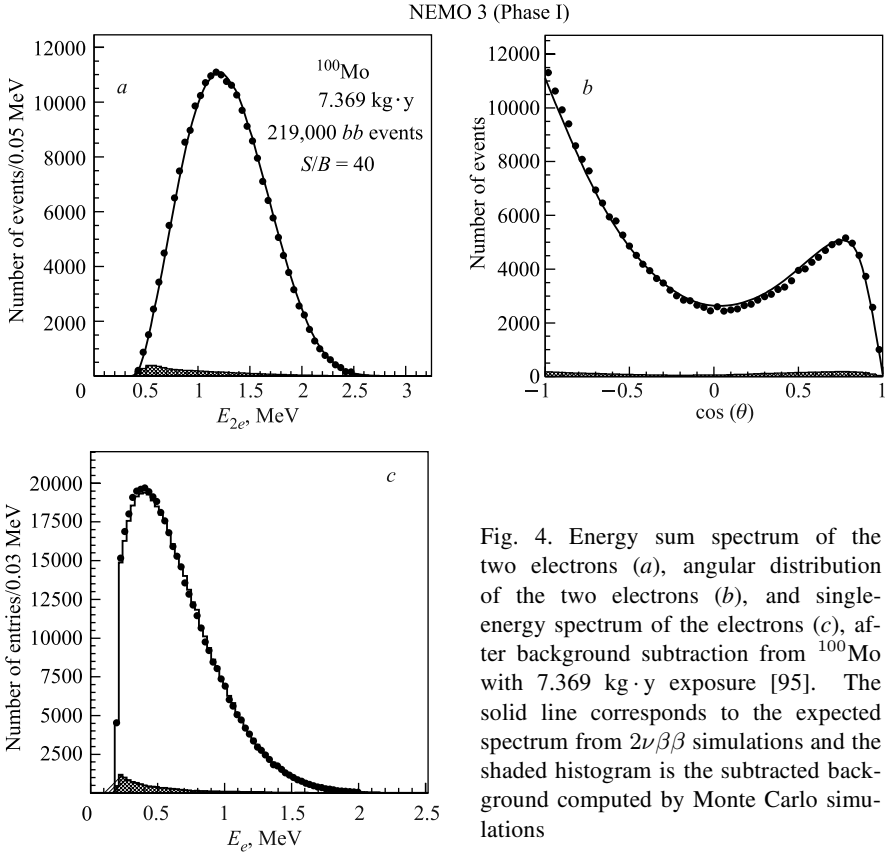

Fig. 4. Energy sum spectrum of the two electrons (*a*), angular distribution of the two electrons (*b*), and single-energy spectrum of the electrons (*c*), after background subtraction from ^{100}Mo with 7.369 kg · y exposure [95]. The solid line corresponds to the expected spectrum from $2\nu\beta\beta$ simulations and the shaded histogram is the subtracted background computed by Monte Carlo simulations

the calculated values of the detection efficiencies for $2\nu\beta\beta$ events, the following half-life values were obtained for ^{100}Mo and ^{82}Se [95]:

$$T_{1/2}(^{100}\mathrm{Mo}; 2\nu) = [7.11 \pm 0.02(\mathrm{stat.}) \pm 0.54(\mathrm{syst.})] \cdot 10^{18}\ \mathrm{y}, \qquad (10)$$

$$T_{1/2}(^{82}\mathrm{Se}; 2\nu) = [9.6 \pm 0.3(\mathrm{stat.}) \pm 1.0(\mathrm{syst.})] \cdot 10^{19}\ \mathrm{y}. \qquad (11)$$

These results and results for ^{48}Ca, ^{96}Zr, ^{116}Cd, ^{130}Te, and ^{150}Nd are presented in Table 8. Notice that the values for ^{100}Mo and ^{116}Cd have been obtained on the assumption that the single-state dominance (SSD) mechanism is valid* [72, 100]. Systematic uncertainties can be decreased using calibrations and can be improved by up to $\sim$ (3–5)%.

*Validity of SSD mechanism in ^{100}Mo was demonstrated using analysis of the single-electron spectrum (see [97, 99]). In the case of ^{116}Cd this is still a hypothesis.

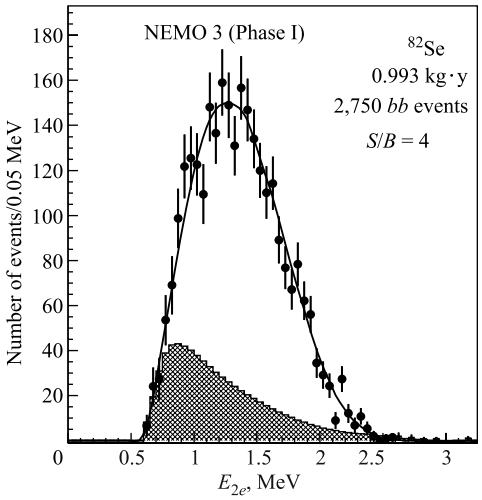

Fig. 5. Energy sum spectrum of the two electrons after background subtraction from ^{82}Se with 0.993 kg · y exposure (the same legend as Fig. 4) [95]. The signal contains 2,750 2β events and the signal-to-background ratio is 4

Table 8. **Two-neutrino half-life values for different nuclei obtained in the NEMO-3 experiment (for ^{116}Cd, ^{48}Ca, and ^{130}Te the results are preliminary). The first error is statistical and the second is systematic; S/B is the signal-to-background ratio**

Isotope	Measurement time, days	Number of 2ν events	S/B	$T_{1/2}(2\nu)$, y
^{100}Mo	389	219000	40	$(7.11 \pm 0.02 \pm 0.54) \cdot 10^{18}$ [95]
^{82}Se	389	2750	4	$(9.6 \pm 0.3 \pm 1.0) \cdot 10^{19}$ [95]
^{116}Cd	1222	6949	10	$(2.88 \pm 0.04 \pm 0.16) \cdot 10^{19}$
^{96}Zr	1221	428	1	$(2.35 \pm 0.14 \pm 0.19) \cdot 10^{19}$ [54]
^{150}Nd	939	2018	2.8	$(9.2^{+0.25}_{-0.22} \pm 0.62) \cdot 10^{18}$ [53]
^{48}Ca	943.16	116	6.8	$(4.4^{+0.5}_{-0.4} \pm 0.4) \cdot 10^{19}$
^{130}Te	1152	236	0.35	$(6.9 \pm 0.9 \pm 1.0) \cdot 10^{20}$

Figure 6 shows the tail of the two-electron energy sum spectrum in the $0\nu\beta\beta$-energy window for ^{100}Mo and ^{82}Se (Phase I+II; 3.75 y of measurement). One can see that the experimental spectrum is in good agreement with the calculated spectrum, which was obtained taking into account all sources of background. Using a maximum likelihood method, the following limits on neutrinoless double-beta decay of ^{100}Mo and ^{82}Se (mass mechanism; 90% CL) have been obtained:

$$T_{1/2}(^{100}\mathrm{Mo}; 0\nu) > 1.1 \cdot 10^{24} \text{ y}, \tag{12}$$

$$T_{1/2}(^{82}\mathrm{Se}; 0\nu) > 3.6 \cdot 10^{23} \text{ y}. \tag{13}$$

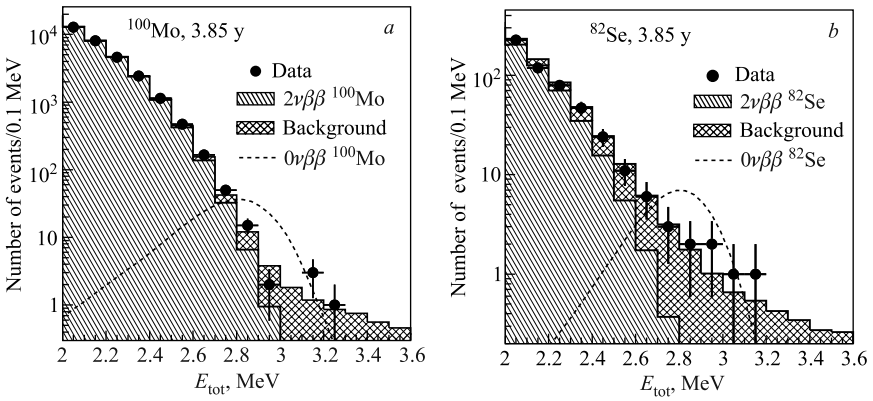

Fig. 6. Distribution of the energy sum of two electrons in the region around $Q_{\beta\beta}$ value for ^{100}Mo (*a*) and ^{82}Se (*b*), 1409 d data [44]. High energy tail of the energy sum distribution for events in molybdenum (*a*) and selenium (*b*) foils are shown with black points. The background contributions are shown within the histogram. The shape of a hypothetical 0ν signal is shown by the curve in arbitrary units

Additionally, using NME values from [7–10] the bound on $\langle m_\nu \rangle$ gives 0.45–0.93 eV for ^{100}Mo and 0.89–1.61 eV for ^{82}Se.

In this experiment the best present limits on all possible modes of double-beta decay with Majoron emission have been obtained, too (see Tables 3 and 4).

NEMO-3 experiment will be running up to the end of 2010.

3. PLANNED EXPERIMENTS

Here seven of the most developed and promising experiments which can be realized within the next few years are discussed (see Table 9). The estimation of the sensitivity in the experiments is made using NMEs from [7–10, 39].

3.1. CUORE [43, 101]. This experiment will be run at the Gran Sasso Underground Laboratory (Italy; 3500 m w.e.). The plan is to investigate 760 kg of $^{\rm nat}TeO_2$, with a total of $\sim$ 200 kg of ^{130}Te. One thousand low-temperature ($\sim$ 8 mK) detectors, each having a weight of 750 g, will be manufactured and arranged in 19 towers. One tower is approximately equivalent to the CUORICINO detector [43]. Planned energy resolution is 5 keV (FWHM). One of the problems here is to reduce the background level by a factor of about 10 to 100 in relation to the background level achieved in the detector CUORICINO. Upon reaching a background level of 0.001 $\mathrm{keV}^{-1} \cdot \mathrm{kg}^{-1} \cdot \mathrm{y}^{-1}$, the sensitivity of the experiment to the 0ν decay of ^{130}Te for 5 y of measurements and at 90% CL will become approximately $6.5 \cdot 10^{26}$ y ($\langle m_\nu \rangle \sim$ 0.02–0.05 eV). For more realistic level of

Table 9. **Seven most developed and promising projects. Sensitivity at 90% CL for three (1st step of GERDA and MAJORANA, SNO+, and KamLAND-Xe) five (EXO, SuperNEMO and CUORE) and ten (full-scale GERDA and MAJORANA) years of measurements is presented.** M **— mass of isotopes**

Experiment	Isotope	M, kg	Sensitivity $T_{1/2}$, y	Sensitivity $\langle m_\nu \rangle$, meV	Status
CUORE [43, 101]	^{130}Te	200	$6.5 \cdot 10^{26*}$ $2.1 \cdot 10^{26**}$	20–50 35–90	In progress
GERDA [102]	^{76}Ge	40 1000	$2 \cdot 10^{26}$ $6 \cdot 10^{27}$	70–300 10–40	In progress R&D
MAJORANA [105, 106]	^{76}Ge	30–60 1000	$(1–2)\cdot 10^{26}$ $6 \cdot 10^{27}$	70–300 10–40	In progress R&D
EXO [107]	^{136}Xe	200 1000	$6.4 \cdot 10^{25}$ $8 \cdot 10^{26}$	95–220 27–63	In progress R&D
SuperNEMO [109–111]	^{82}Se	100–200	$(1–2)\cdot 10^{26}$	40–110	In progress
KamLAND-Xe [113]	^{136}Xe	400	$4.5\cdot 10^{26}$	40–80	In progress
SNO+ [112]	^{150}Nd	56 500	$\sim 4.5\cdot 10^{24}$ $\sim 3\cdot 10^{25}$	100–300 40–120	In progress R&D

*For the background 0.001 $\text{keV}^{-1} \cdot \text{kg}^{-1} \cdot \text{y}^{-1}$.
**For the background 0.01 $\text{keV}^{-1} \cdot \text{kg}^{-1} \cdot \text{y}^{-1}$.

background 0.01 $\text{keV}^{-1} \cdot \text{kg}^{-1} \cdot \text{y}^{-1}$ sensitivity will be $\sim 2.1 \cdot 10^{26}$ y for half-life and $\sim$ 0.04–0.09 eV for the effective Majorana neutrino mass. The experiment has been approved and funded. A general test of the CUORE detector, comprising a single tower and named CUORE-0, will take data in 2011.

3.2. GERDA [102]. This is one of two planned experiments with ^{76}Ge (along with the MAJORANA experiment). The experiment is to be located in the Gran Sasso Underground Laboratory (Italy, 3500 m w.e.). The proposal is based on ideas and approaches which were proposed for GENIUS [16] and the GEM [103] experiments. The plan is to place «naked» HPGe detectors in highly purified liquid argon (as passive and active shield). It minimizes the weight of construction material near the detectors and decreases the level of background. The liquid argon dewar is placed into a vessel of very pure water. The water plays a role of passive and active (Cherenkov radiation) shield.

The proposal involves three phases. In the first phase, the existing HPGe detectors ($\sim$ 18 kg), which previously were used in the Heidelberg–Moscow [41] and IGEX [42] experiments, will be utilized. In the second phase $\sim$ 40 kg of

enriched Ge will be investigated. In the third phase the plan is to use $\sim$ 500–1000 kg of ^{76}Ge.

The first phase, lasting one year, is to measure with a sensitivity of $3 \cdot 10^{25}$ y, that gives a possibility of checking the «positive» result of [32–34]. The sensitivity of the second phase (for three years of measurements) will be $\sim 2 \cdot 10^{26}$ y. This corresponds to a sensitivity for $\langle m_\nu \rangle$ at the level of $\sim$ 0.07–0.3 eV.

The first two phases have been approved and funded. The first-phase setup is in an advanced construction stage and data taking is foreseen for 2011. The results of this first step will play an important role in the decision to support the full scale experiment.

The project is very promising although it will be difficult to reach the desired level of background. One of the significant problems is ^{222}Rn in the liquid argon (see, for example, results of [104]) and, in addition, background from ^{42}Ar can be a problem, too.

3.3. MAJORANA [105, 106]. The MAJORANA facility will consist of $\sim$ 1000 HPGe detectors manufactured from enriched germanium (the degree of enrichment is $> 86\%$). The total mass of enriched germanium will be 1000 kg. The facility is designed in such a way that it will consist of many individual supercryostats manufactured from low radioactive copper, each containing HPGe detectors. The entire facility will be surrounded by a passive shield and will be located at an underground laboratory in the United States. Only the total energy deposition will be utilized in measuring the $0\nu\beta\beta$ decay of ^{76}Ge to the ground state of the daughter nucleus. The use of HPGe detectors, pulse shape analysis, anticoincidence, and low radioactivity structural materials will make it possible to reduce the background to a value below $3 \cdot 10^{-4}$ keV$^{-1} \cdot$kg$^{-1} \cdot$y^{-1} and to reach a sensitivity of about $6 \cdot 10^{27}$ y within ten years of measurements. The corresponding sensitivity to the effective mass of the Majorana neutrino is about 0.01 to 0.04 eV. The measurement of the $0\nu\beta\beta$ decay of ^{76}Ge to the 0^+ excited state of the daughter nucleus will be performed by recording two cascade photons and two beta electrons. The planned sensitivity for this process is about 10^{27} y.

In the first step $\sim$ 30–60 kg of ^{76}Ge will be investigated. It is anticipated that the sensitivity to $0\nu\beta\beta$ decay to the ground state of the daughter nuclei for 3 years of measurements will be $(1-2) \cdot 10^{26}$ y. It will reject or confirm the «positive» result from [32–34]. Sensitivity to $\langle m_\nu \rangle$ will be $\sim$ 0.07–0.3 eV. During this time different methods and technical questions will be checked and possible background problems will be investigated. The first module of MAJORANA (DEMONSTRATOR) is under construction now and measurements are planned to begin in 2013.

3.4. EXO [107]. In this experiment the plan is to implement Moe's proposal of 1991 [108]. Specifically it is to record both ionization electrons and the Ba^+

ion originating from the double-beta-decay process ^{136}Xe $\rightarrow^{136}$ Ba$^{++} + 2e^-$. In [107], it is proposed to operate with 1 t of ^{136}Xe. The actual technical implementation of the experiment has not yet been developed. One of the possible schemes is to fill a TPC with liquid enriched xenon. To avoid the background from the 2ν decay of ^{136}Xe, the energy resolution of the detector must not be poorer than 3.8% (FWHM) at an energy of 2.5 MeV (ionization and scintillation signals will be detected).

In the 0ν decay of ^{136}Xe, the TPC will measure the energy of two electrons and the coordinates of the event to within a few millimeters. After that, using a special stick, Ba ions will be removed from the liquid and then will be registered in a special cell by resonance excitation. For Ba^{++} to undergo a transition to a state of Ba$^+$, a special gas is added to xenon. The authors of the project assume that the background will be reduced to one event within five years of measurements. Given a 70% detection efficiency it will be possible to reach a sensitivity of about $8{\cdot}^{26}$ y for the ^{136}Xe half-life and a sensitivity of about 0.03 to 0.06 eV for the neutrino mass.

One should note that the principle difficulty in this experiment is associated with detecting the Ba$^+$ ion with a reasonably high efficiency. This issue calls for thorough experimental tests, and positive results have yet to be obtained.

As the first stage of the experiment EXO-200 will use 200 kg of ^{136}Xe without Ba ion identification. This experiment is currently under preparation and measurements will start probably in 2011. The 200 kg of enriched Xe is a product of Russia with an enrichment of $\sim 80\%$. If the background is 40 events in 5 y of measurements, as estimated by the authors, then the sensitivity of the experiment will be $\sim 6 \cdot 10^{25}$ y. This corresponds to sensitivity for $\langle m_\nu \rangle$ at the level $\sim 0.1{-}0.2$ eV. This initial prototype will operate at the Waste Isolation Pilot Plant (WIPP) in Southern New Mexico (USA).

3.5. SuperNEMO [109–111]. The NEMO Collaboration has studied and is pursuing an experiment that will observe 100–200 kg of ^{82}Se with the aim of reaching a sensitivity for the 0ν decay mode at the level of $T_{1/2} \sim (1{-}2) \cdot 10^{26}$ y. The corresponding sensitivity to the neutrino mass is 0.04 to 0.11 eV. In order to accomplish this goal, it is proposed to use the experimental procedures nearly identical to that in the NEMO-3 experiment (see Subsec 2.1). The new detector will have planar geometry and will consist of 20 identical modules (5–7 kg of ^{82}Se in each sector). A ^{82}Se source having a thickness of about 40 mg/cm^2 and a very low content of radioactive admixtures is placed at the center of the modules. The detector will again record all features of double-beta decay: the electron energy will be recorded by counters based on plastic scintillators ($\Delta E/E \sim 8{-}10\%$ (FWHM) at $E = 1$ MeV), while tracks will be reconstructed with the aid of Geiger counters. The same device can be used to investigate ^{150}Nd, ^{100}Mo, ^{116}Cd, and ^{130}Te with a sensitivity to $0\nu\beta\beta$ decay at a level of about $(0.5{-}1) \cdot 10^{26}$ y.

The use of an already tested experimental technique is an appealing feature of this experiment. The plan is to arrange the equipment at the new Frejus Underground Laboratory (France; the respective depth being 4800 m w.e.). The construction and commissioning of the Demonstrator (first module) will be completed in 2013.

3.6. SNO+. SNO+ is an upgrade of the solar neutrino experiment SNO (Canada), aiming at filling the SNO detector with Nd-loaded liquid scintillator to investigate the isotope ^{150}Nd [112]. The present plan is to use 0.1% natural Nd-loaded liquid scintillator in 1000 t, providing a source of 56 kg ^{150}Nd. SNO+ is in construction phase with natural neodymium. Data taking is foreseen in 2012. After 3 y of data taking sensitivity will be $\sim 4.5 \cdot 10^{24}$ y (or $0.1-0.3$ eV for $\langle m_\nu \rangle$). Finally 500 kg of enriched ^{150}Nd will be used (if enrichment of such quantity of Nd will be possible). Planned sensitivity is $\sim 3 \cdot 10^{25}$ y.

3.7. KamLAND-Xe. KamLAND-Xe is an upgrade of the KamLAND setup [113]. The idea is to convert it to neutrinoless double-beta decay search by dissolving Xe gas in the liquid scintillator. This approach was proposed by R. Raghavan in 1994 [114]. This mixture (400 kg of Xe in 16 t of liquid scintillator) will be contained in a small balloon suspended in the centre of the KamLAND sphere. It will guarantee low background level and high sensitivity of this experiment (see Table 9). The programme should start in 2011 (first phase) with 400 kg of isotope and continue in 2013 (2015) with 1 ton of xenon enriched to 90% in ^{136}Xe.

CONCLUSIONS

In conclusion, two-neutrino double-beta decay has so far been recorded for ten nuclei (^{48}Ca, ^{76}Ge, ^{82}Se, ^{96}Zr, ^{100}Mo, ^{116}Cd, ^{128}Te, ^{130}Te, ^{150}Nd, ^{238}U). In addition, the $2\beta(2\nu)$ decay of ^{100}Mo and ^{150}Nd to the 0^+ excited state of the daughter nucleus has been observed and the ECEC(2ν) process in ^{130}Ba was observed. Experiments studying two-neutrino double-beta decay are presently approaching a qualitatively new level, where high-precision measurements are performed not only for half-lives but also for all other parameters of the process. As a result, a trend is emerging toward thoroughly investigating all aspects of two-neutrino double-beta decay, and this will furnish very important information about the values of NME, the parameters of various theoretical models, and so on. In this connection, one may expect advances in the calculation of NME and in the understanding of the nuclear physics aspects of double-beta decay.

Neutrinoless double-beta decay has not yet been confirmed. There is a conservative limit on the effective value of the Majorana neutrino mass at the level of 0.75 eV.

The next-generation experiments, where the mass of the isotopes being studied will be as grand as 100 to 1000 kg, will have started within a few years. In all probability, they will make it possible to reach the sensitivity for the neutrino mass at a level of 0.01 to 0.1 eV. First step of GERDA (18 kg of ^{76}Ge), EXO-200 (200 kg of ^{136}Xe), CUORE-0 ($\sim$ 40 kg of natural Te), and KamLAND-Xe (400 kg of ^{136}Xe) plan to start data-tacking in 2011.

Acknowledgements. This work was supported by Russian Federal Agency for Atomic Energy.

REFERENCES

1. *Valle J. W. F.* // J. Phys. Conf. Ser. 2006. V. 53. P. 473; AIP Conf. Proc. 2009. V. 1115. P. 13.
2. *Bilenky S. M.* // J. Phys. A. 2007. V. 40. P. 6707.
3. *Mohapatra R. N., Smirnov A. Y.* // Ann. Rev. Nucl. Part. Sci. 2006. V. 56. P. 569.
4. *Pascoli S., Petcov S. T., Rodejohann W.* // Phys. Lett. B. 2003. V. 558. P. 141.
5. *Mohapatra R. N. et al.* hep-ph/0510213.
6. *Pascoli S., Petcov S. T., Schwetz T.* // Nucl. Phys. B. 2006. V. 734. P. 24.
7. *Rodin V. A. et al.* // Nucl. Phys. A. 2006. V. 766. P. 107; 2007. V. 793. P. 213.
8. *Kortelainen M., Suhonen J.* // Phys. Rev. C. 2007. V. 75. P. 051303(R).
9. *Kortelainen M., Suhonen J.* // Ibid. V. 76. P. 024315.
10. *Simkovic F. et al.* // Phys. Rev. C. 2008. V. 77. P. 045503.
11. *Barabash A. S.* // JETP Lett. 1998. V. 68. P. 1.
12. *Barabash A. S.* // Eur. Phys. J. A. 2000. V. 8. P. 137.
13. *Barabash A. S.* // Astrophys. Space Sci. 2003. V. 283. P. 169.
14. *Dolgov A. D., Smirnov A. Yu.* // Phys. Lett. B. 2005. V. 621. P. 1.
15. *Barabash A. S. et al.* // Nucl. Phys. B. 2007. V. 783. P. 90.
16. *Klapdor-Kleingrothaus H. V., Hellmig J., Hirsch M.* // J. Phys. G. 1998. V. 24. P. 483.
17. *Gelmini G. B., Roncadelli M.* // Phys. Lett. B. 1981. V. 99. P. 411.
18. *Caso C. et al. (Particle Data Group)* // Eur. Phys. J. C. 1998. V. 3. P. 1.
19. *Mohapatra R. N., Pal P. B.* Massive Neutrinos in Physics and Astrophysics. Singapore: World Sci., 1991.
20. *Berezhiani Z. G., Smirnov A. Yu., Valle J. W. F.* // Phys. Lett. B. 1992. V. 291. P. 99.
21. *Mohapatra R. N., Takasugi E.* // Phys. Lett. B. 1988. V. 211. P. 192.
22. *Burgess C. P., Cline J. M.* // Phys. Lett. B. 1993. V. 298. P. 141; Phys. Rev. D. 1994. V. 49. P. 5925.
23. *Bamert P., Burgess C.Ṕ., Mohapatra R. N.* // Nucl. Phys. B. 1995. V. 449. P. 25.
24. *Carone C.D̀.* // Phys. Lett. B. 1993. V. 308. P. 85.
25. *Mohapatra R. N., Perez-Lorenzana A., Pires C.Ȧ. S.* // Phys. Lett. B. 2000. V. 491. P. 143.
26. *Tretyak V. I., Zdesenko Yu. G.* // At. Data Nucl. Data Tables. 2002. V. 80. P. 83.
27. *Inghram M. G., Reynolds J. H.* // Phys. Rev. 1950. V. 78. P. 822.
28. *Kirsten T., Gentner W., Schaeffer O. A.* // Z. Phys. A. 1967. V. 202. P. 273.

29. *Elliott S. R., Hahn A. A., Moe M. K.* // Phys. Rev. Lett. 1987. V. 59. P. 2020.
30. *Barabash A. S.* // Phys. Rev. C. 2010. V. 81. P. 035501.
31. *Turkevich A. L., Economou T. E., Cowan G. A.* // Phys. Rev. Lett. 1991. V. 67. P. 3211.
32. *Klapdor-Kleingrothaus H. V. et al.* // Phys. Lett. B. 2004. V. 586. P. 198.
33. *Klapdor-Kleingrothaus H. V. et al.* // Mod. Phys. Lett. A. 2006. V. 21. P. 1547.
34. *Klapdor-Kleingrothaus H. V. et al.* // Mod. Phys. Lett. A. 2001. V. 16. P. 2409.
35. *Bakalyarov A. M. et al.* // Phys. Part. Nucl. Lett. 2005. V. 2. P. 77; hep-ex/0309016.
36. *Aalseth C. E. et al.* // Mod. Phys. Lett. A. 2002. V. 17. P. 1475.
37. *Zdesenko Yu. G., Danevich F. A., Tretyak V. I.* // Phys. Lett. B. 2002. V. 546. P. 206.
38. *Strumia A., Vissani F.* // Nucl. Phys. B. 2005. V. 726. P. 294.
39. *Caurier E. et al.* // Phys. Rev. Lett. 2008. V. 100. P. 052503.
40. *Caurier E., Nowacki F., Poves A.* // Intern. J. Mod. Phys. E. 2007. V. 16. P. 552.
41. *Klapdor-Kleingrothaus H. V. et al.* // Eur. Phys. J. A. 2001. V. 12. P. 147.
42. *Aalseth C. E. et al.* // Phys. Rev. D. 2002. V. 65. P. 092007.
43. *Arnaboldi C. et al.* // Phys. Rev. C. 2008. V. 78. P. 035502.
44. *Barabash A. S., Brudanin V. B.* nucl-ex/1002.2862.
45. *Bernabei R. et al.* // Phys. Lett. B. 2002. V. 546. P. 23.
46. *Danevich F. A. et al.* // Phys. Rev. C. 2003. V. 68. P. 035501.
47. *Arnold R. et al.* // Nucl. Phys. A. 2006. V. 765. P. 483.
48. *Manuel O. K.* // J. Phys. G. 1991. V. 17. P. S221.
49. *Gunther M. et al.* // Phys. Rev. D. 1997. V. 55. P. 54.
50. *Arnold R. et al.* // Nucl. Phys. A. 2000. V. 678. P. 341.
51. *Tanaka J., Ejiri H.* // Phys. Rev. D. 1993. V. 48. P. 5412.
52. *Arnaboldi C. et al.* // Phys. Lett. B. 2003. V. 557. P. 167.
53. *Argyriades J. et al.* // Phys. Rev. C. 2009. V. 80. P. 032501(R).
54. *Arnold R. et al.* // Nucl. Phys. A. 2010. V. 847. P. 168.
55. *Barabash A. S.* // Phys. At. Nucl. 2010. V. 73. P. 162.
56. *Suhonen J., Aunola M.* // Nucl. Phys. A. 2003. V. 723. P. 271.
57. *Hirsch M. et al.* // Z. Phys. A. 1994. V. 347. P. 151.
58. *Doi M., Kotani T.* // Prog. Theor. Phys. 1993. V. 89. P. 139.
59. *Sujkowski Z., Wycech S.* // Phys. Rev. C. 2004. V. 70. P. 052501(R).
60. *Vergados J. D.* // Nucl. Phys. B. 1983. V. 218. P. 109.
61. *Barabash A. S.* // JETP Lett. 1994. V. 59. P. 677.
62. *Meshik A. P. et al.* // Phys. Rev. C. 2001. V. 64. P. 035205.
63. *Gavriljuk Ju. M. et al.* nucl-ex/1006.5133.
64. *Rukhadze N. I. et al.* // J. Phys. Conf. Ser. 2010. V. 203. P. 012072.
65. *Barabash A. S. et al.* // J. Phys. G. 2007. V. 34. P. 1721.
66. *Wilson J. R.* // Czech. J. Phys. 2006. V. 56. P. 543.
67. *Barabash A. S. et al.* // Nucl. Phys. A. 2007. V. 785. P. 371.
68. *Belli P. et al.* // Phys. Lett. B. 2008. V. 658. P. 193.
69. *Kim H.J. et al.* // Nucl. Phys. A. 2007. V. 793. P. 171.
70. *Barabash A. S. et al.* // Nucl. Phys. A. 2008. V. 807. P. 269.

71. *Dawson J. et al.* // Ibid. V. 799. P. 167.
72. *Domin P. et al.* // Nucl. Phys. A. 2005. V. 753. P. 337.
73. *Shukla A. et al.* // Eur. Phys. J. A. 2005. V. 23. P. 235.
74. *Raina P. K. et al.* // Eur. Phys. J. A. 2006. V. 28. P. 27.
75. *Shukla A., Raina P. K., Rath P. K.* // J. Phys. G. 2007. V. 34. P. 549.
76. *Mishra S. et al.* // Phys. Rev. C. 2008. V. 78. P. 024307.
77. *Rath P. K. et al.* // Phys. Rev. C. 2009. V. 80. P. 044303.
78. *Shukla A., Sahu R., Kota V. K. B.* // Ibid. V. 80. P. 057305.
79. *Barabash A. S., Saakyan R. R.* // Phys. At. Nucl. 1996. V. 59. P. 179.
80. *Saenz C. et al.* // Phys. Rev. C. 1994. V. 50. P. 1170.
81. *Vasil'ev S. I. et al.* // JETP Lett. 1993. V. 57. P. 320.
82. *Belli P. et al.* // Astropart. Phys. 1999. V. 10. P. 115.
83. *Barabash A. S. et al.* // Z. Phys. A. 1997. V. 357. P. 351.
84. *Winter R. G.* // Phys. Rev. 1955. V. 100. P. 142.
85. *Voloshin M. B., Misel'makher G. V., Eramzhyan R. A.* // JETP Lett. 1982. V. 35. P. 656.
86. *Bernabeu J. et al.* // Nucl. Phys. B. 1983. V. 223. P. 15.
87. *Rahaman S. et al.* // Phys. Rev. Lett. 2009. V. 103. P. 042501.
88. *Mount B. J., Redshaw M., Myers E. G.* // Phys. Rev. C. 2010. V. 81. P. 032501R.
89. *Kolhinen V. S. et al.* // Phys. Lett. B. 2010. V. 684. P. 17.
90. *Belli P. et al.* // Eur. Phys. J. A. 2009. V. 42. P. 171.
91. *Belli P. et al.* // Nucl. Phys. A. 2009. V. 824. P. 101.
92. *Dawson J. et al.* // Phys. Rev. C. 2008. V. 78. P. 035503.
93. *Kidd M. F., Esterline J. H., Tornow W.* // Ibid. P. 035504.
94. *Barabash A. S. et al.* // Phys. Rev. C. 2009. V. 80. P. 035501.
95. *Arnold R. et al.* // Phys. Rev. Lett. 2005. V. 95. P. 182302.
96. *Arnold R. et al.* // Nucl. Instr. Meth. A. 2005. V. 536. P. 79.
97. *Arnold R. et al.* // JETP Lett. 2004. V. 80. P. 377.
98. *Arnold R. et al.* // Nucl. Instr. Meth. A. 1995. V. 354. P. 338.
99. *Shitov Yu. A.* // Phys. At. Nucl. 2006. V. 69. P. 2090.
100. *Simkovic F., Domin P., Semenov S.* // J. Phys. G. 2001. V. 27. P. 2233.
101. *Arnaboldi C. et al.* // Nucl. Instr. Meth. A. 2004. V. 518. P. 775.
102. *Abt I. et al.* hep-ex/0404039.
103. *Zdesenko Yu. G., Ponkratenko O. A., Tretyak V. I.* // J. Phys. G. 2001. V. 27. P. 2129.
104. *Klapdor-Kleingrothaus H. V. et al.* // Nucl. Instr. Meth. A. 2004. V. 530. P. 410.
105. *Majorana Collab.* nucl-ex/0311013.
106. *Avignone F.T.* // Prog. Part. Nucl. Phys. 2010. V. 64. P. 258.
107. *Danilov M. et al.* // Phys. Lett. B. 2000. V. 480. P. 12.
108. *Moe M.* // Phys. Rev. C. 1991. V. 44. P. R931.
109. *Barabash A. S.* // Czech. J. Phys. 2002. V. 52. P. 575.
110. *Barabash A. S.* // Phys. At. Nucl. 2004. V. 67. P. 1984.
111. *Saakyan R.* // J. Phys. Conf. Ser. 2009. V. 179. P. 012006.
112. *Kraus C., Peeters S. J. M.* // Prog. Part. Nucl. Phys. 2010. V. 64. P. 273.
113. *Nakamura K.* Report on Intern. Conf. «Neutrino'2010», Athens, 2010.
114. *Raghavan R. S.* // Phys. Rev. Lett. 1994. V. 72. P. 1411.